

Stabilizing non-covalent interactions of ligand aromatic moieties and proline in ligand–protein systems

Milena Jovanović · Maja Gruden-Pavlović ·
Mario Zlatović

Received: 11 October 2013 / Accepted: 10 November 2014 / Published online: 20 December 2014
© Springer-Verlag Wien 2014

Abstract Proline, due to its conformational specificity, is known to show some unique properties and has significant functions in the tertiary structure of proteins. It was suggested that proline could have an important influence on some vital interactions in protein as well, by engaging in non-covalent stabilization interactions with some aromatic moieties. In this work, the interactions that occur between proline and some aromatic moieties in ligands were investigated by means of the density functional theory using an exchange–correlation functional capable of taking into account dispersion interactions. The obtained results showed that the stabilization energy between a properly placed proline and an aromatic moiety could be as large as 25 kJ/mol and hence be a significant factor in placing a ligand in binding site of a protein. This indicates that the error in determining the most favorable structure of ligand–protein complexes obtained by usual molecular docking experiments sometimes could be the result of neglecting this type of interactions.

Keywords Ab initio calculations · Non-covalent interactions · Proteins · Molecular modeling · Density functional theory

Electronic supplementary material The online version of this article (doi:10.1007/s00706-014-1357-8) contains supplementary material, which is available to authorized users.

M. Jovanović · M. Gruden-Pavlović · M. Zlatović (✉)
Faculty of Chemistry, University of Belgrade,
Studentski trg 12-16, 11000 Belgrade, Serbia
e-mail: mario@chem.bg.ac.rs

Introduction

Proline, as the only amino acid with a cyclic pyrrolidine structure that involves an α -amino group, plays a distinctive role in determining the structure and function of proteins. The conformational rigidity of proline, due to significantly lower ΔS during protein folding when compared to other amino acids, is believed to play an important role in stabilizing the tertiary structure of proteins [1]. Moreover, in the secondary structure of proteins, the general opinion is that proline is one of the most potent alpha-helix disruptors in water-soluble globular proteins and in transmembrane alpha helices of transmembrane proteins [2, 3]. On the other hand, some results show that proline is a better helix former than alanine when it is the first residue at the N-terminus on an alpha helix [4]. In transmembrane transport proteins, proline residues are important for substrate binding and recognition [5].

However, the importance and uniqueness of proline does not end here. Some authors suggested that proline can have significant impacts on the stabilization of both protein–protein and protein–ligand interactions [6, 7]. Riley et al. [6] in their computational studies of human carbonic anhydrase II calculated that the phenyl ring of the inhibitor interacts with the pyrrolidine ring of proline in a manner similar to its interaction with the aromatic moiety of phenylalanine. Hobza and coworkers studied interactions between proline and aromatic side chains of amino acids in a polypeptide model taken from the structure of the Trp-cage (PDB code 1L2Y [8]) and showed by quantum mechanical calculations that, in the case of parallel alignment of the aromatic part of Trp and the proline ring, significant interacting forces can be found, which are mostly dispersive in nature (with some electrostatic part).

These results show that proline interactions can play an important role in biomolecules such as proteins. Unfortunately, because of size and the need for sustainable calculations, in computational studies of biomolecules, especially when a larger number of structures are involved, calculations are usually limited to the molecular mechanic (MM) method. In such situations, our results, e.g. poses from docking simulations, are as good as our force field (FF) parameters are. There has been a noticeable advance in parameterization of some modern type FFs, which include numerous descriptions of a variety of non-bonded interactions [9] and more parameterized functions are included to improve the performance and ability of MM methods to correctly describe large systems, especially bioactive molecules [10]. Nevertheless, some special types of non-covalent interactions, such as those with proline, can still be underestimated and strongly depend on the parameterization procedure. Bearing previous calculations in mind [6, 7], we believe that such interactions could influence the binding strength and binding positions of ligands in a biomolecule. In biosystems where proline is conveniently placed near an aromatic system, this type of bonding, if neglected, could lead to false predictions of activity or to incorrect docking positions, if just docking scores are relied upon.

To show the possible magnitudes of interactions of proline with some aromatic rings, it was decided to calculate the strength of these non-covalent interactions using *ab initio* calculations on model systems. The goal was to pinpoint the specificity of proline and its importance in ligand binding and positioning. Modern force fields and scoring functions often enable advanced treatment of non-covalent interaction energies, e.g. various π - π interactions. Nevertheless, the specificity of the proline ring and interactions originating from its unique shape and properties can sometimes produce misleading results. Our aim was to examine the specific interactions of proline and aromatic moieties by means of the density functional theory (DFT), to obtain accurate and, moreover, parameter-free results. The accuracy of DFT calculations predominantly depends on the suitability of the approximations made for the XC (exchange correlation) functional and the size of the basis set. Therefore, the influence of different XC functionals (B3LYP, M06-2X, ω B97X-D, B97-D3) and different basis sets for the analysis of the non-covalent interactions of proline with aromatic rings has been investigated.

The intentions were to produce sustainable results with low computer costs and to show that this kind of calculations could be performed in a time comparable to those usual for molecular mechanics calculations to further clarify and improve the results produced by methods regularly used for large biological systems.

Results and discussion

For the purpose of this investigation, two main model systems were selected. The first model system was derived from one of our currently running projects, i.e. investigation of various inhibitors of the light chain of botulinum neurotoxin serotype A (BoNT/A LC) [11]. Molecular docking experiment for one series of ligands, containing the chloroquine moiety produced two main docking poses with a slight difference in the docking score. In one of them, the chloroquine group was in the vicinity of proline Pro239 from the protein chain, with T-shaped ring plains (Fig. 1). We wanted to find if there is some additional non-covalent interaction that could be important for binding, which is not accounted for while using binding simulation techniques like ligand docking.

The coordinates for the second model system were derived from existing crystal structures of proteins with bound ligands. After a thorough inspection of the search results, the tetracycline repressor protein class D complexed with anhydrotetracycline (PDB code 2XPU [12]) was selected. In this structure, the position of proline Pro109 towards the aromatic ligand is somewhat similar to our model (Fig. 2). As this part of the molecule contains no other significant amino acid residues that could stabilize the ligand by non-covalent forces, it was assumed that the given structure could be a model system for the present research.

To perform these calculations, structurally reduced models, containing several aromatic moieties, including chloroquine from our BoNT/A inhibitor (Fig. 3, **A1–A5**) and the reduced structure of proline (Fig. 3, **B**) were employed. The geometries of these models were optimized using the DFT B3LYP [13] functional with 6-311++G(d,p). It is well known that B3LYP

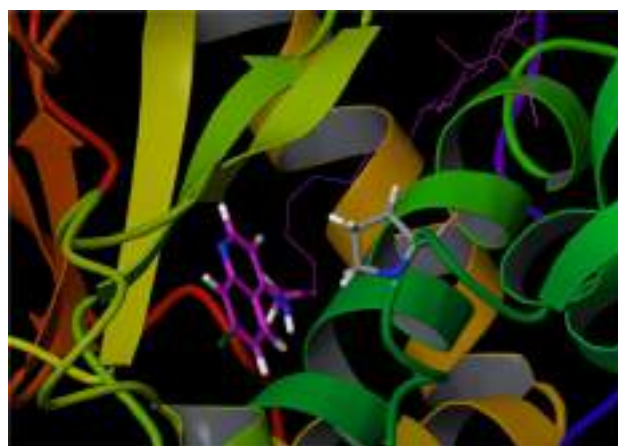


Fig. 1 Aromatic group of BoNT/A LC inhibitor in vicinity of Pro239 in model produced by molecular docking experiments

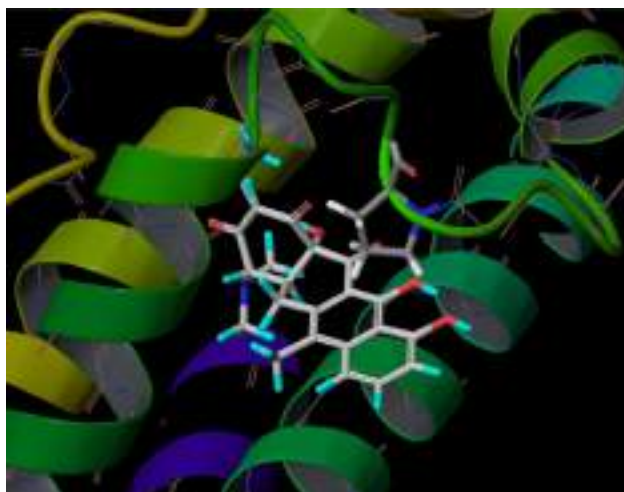


Fig. 2 Crystal structure of 2XPU with anhydrotetracycline

6-311++G(d,p) usually produces good geometries, generally in accordance with calculations on a higher level of theory and with a larger basis set, but in a much shorter time [14].

The optimized monomers were positioned in space to produce dimer structures in such a way that the heavy atom coordinates correspond to the coordinates of the aromatic moiety and Pro239 from our docking pose of the BoNT/A inhibitor in one set and to the coordinates of Pro109 from the crystal structure of 2XPU in the other set. Thus, we produced two sets containing five dimer structures each (1–5 and 6–10, Figs. 4, 5).

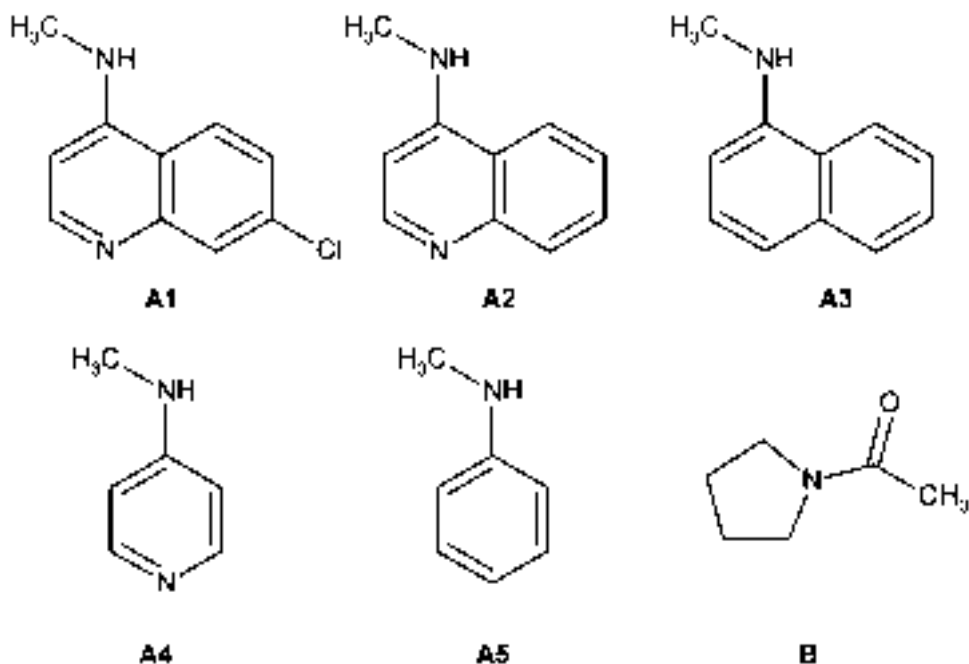
We wanted to elucidate how OPLS-2005 [15], FF used in our docking experiment, treats the interaction of proline with an aromatic ring. The results for the interaction energies of dimers 1–10 (Figs. 4, 5, structures 1–10) calculated by OPLS-2005 FF revealed stabilization by non-covalent interactions for structures 6–10, but for structures 1–5 repulsive forces were calculated (Table 1).

Hence, the energies of the non-covalent interactions for all ten model systems were calculated with different XC functionals and different basis sets. The results of these calculations are reported in Table 1.

Even though B3LYP is one of the most often used DFT functionals, and is accurate for many properties, it is well known that it failed for systems where dispersion forces dominate to play a significant role [16]. The motive for including these results was just to illustrate the size of error when a non-suitable method is used. For all dimers, B3LYP calculations resulted in repulsive interactions. Thus, the results obtained by this functional were not used in the further discussion.

Irrespective of the choice of other XC functionals, the calculations for structure 5 revealed intermolecular repulsive interactions, or a small amount of stabilization in general (Table 1). Another fact is obvious: with a change in the geometry, the stabilization of the non-covalent systems rise significantly, and for the structures 6–10, larger stabilization energies due to non-covalent interactions were obtained than for structures 1–5. Nevertheless, even for systems 1–5, non-negligible stabilization forces (even up to 6–8 kJ/mol) were calculated.

Fig. 3 Structures used for constructing models: **A1**, 7-chloro-*N*-methylquinolin-4-amine; **A2**, *N*-methylquinolin-4-amine; **A3**, *N*-methylnaphthalen-1-amine; **A4**, *N*-methylpyridin-4-amine; **A5**, *N*-methylaniline; **B**, *N*-acetylpyrrolidine



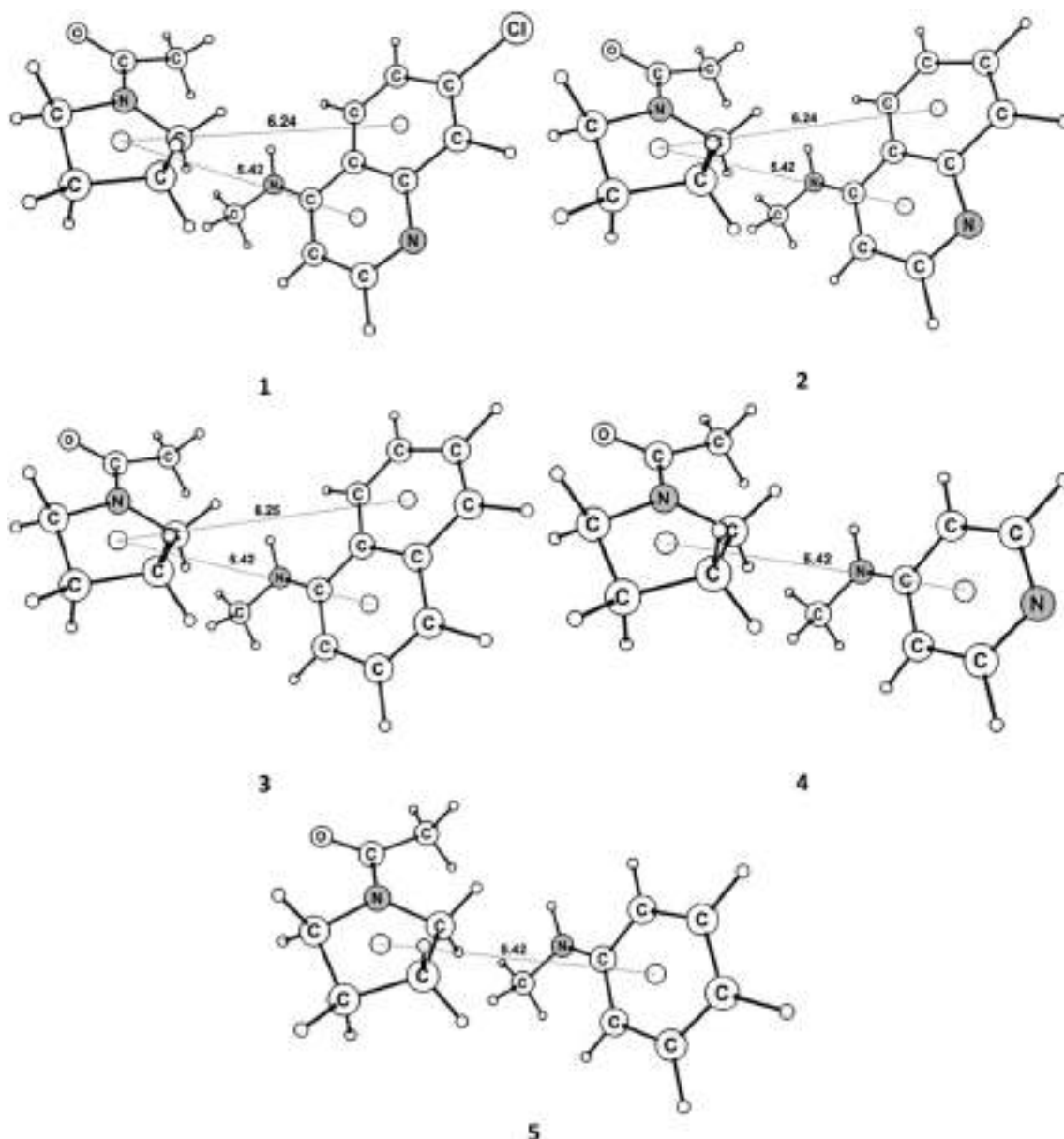


Fig. 4 Structures of non-covalent complexes based on geometries from docking simulations: **1**, A1 and B; **2**, A2 and B; **3**, A3 and B; **4**, A4 and B; **5**, A5 and B (distances in Å)

Results for non-covalent interaction energies differ depending on the method used. Energies produced by ω B97X-D [17] tend to be higher than those produced by M06-2X [18], while energies calculated by B97-D3 are somewhere in the middle. Such behavior is expected as the ω B97X-D functional tends to overestimate, while M06-2X is known to underestimate these interactions [19]. Enlarging the aromatic system to two condensed rings increases the non-covalent interactions, as anticipated. Introducing heteroatoms in an aromatic system, both as a ring member and as a substituent, changes the intermolecular forces in a predictable way. The nitrogen atom introduced in **9** and **7**

decreases the interaction energies when compared to **10** and **8** because of its electron-withdrawing properties. For system **2**, a slightly different behavior could be noticed, as it is slightly more stable than **3**, but this could result from different positioning. In models **1–3**, the proline system is more distant from the second aromatic ring than in **6–8**, hence, the overall influence on the non-covalent forces decreased. A chlorine atom in position **7** slightly decreased the attractive non-covalent forces as well.

Another interesting result could be seen from graphic on which different basis sets are compared (Supplementary Material, Fig. S4), the rather small Pople basis set

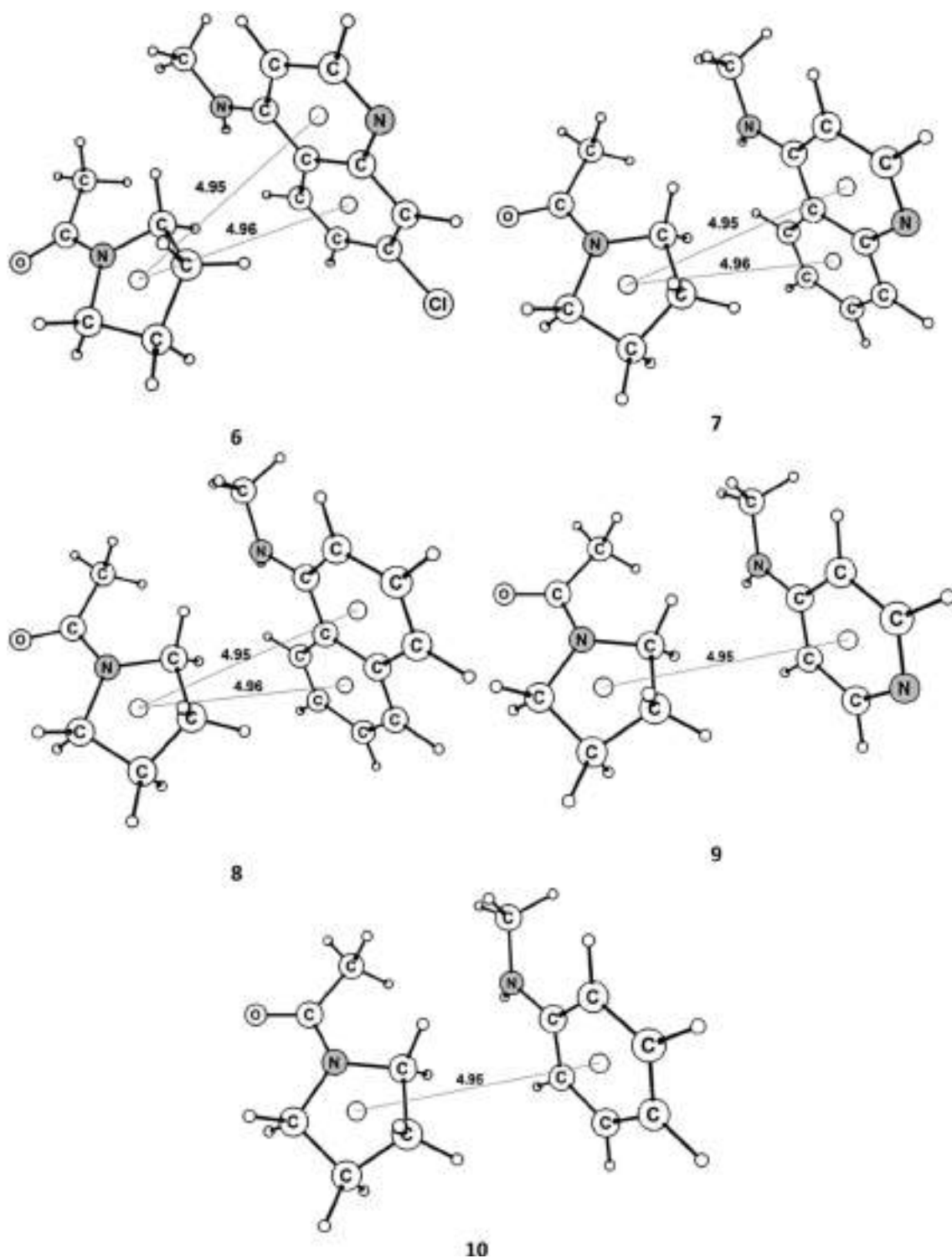


Fig. 5 Structures of non-covalent complexes based on geometries from 2XPU: **6**, A1 and B; **7**, A2 and B; **8**, A3 and B; **9**, A4 and B; **10**, A5 and B (distances in Å)

6-311++G(d,p), the extended 6-311++G(3df,3dp), and the elaborate Dunning aug-cc-pVDZ basis set. It can be seen that the differences in the interaction energies are not large—up to 0.78 kJ/mol between the smallest Pople and

the aug-cc-pVDZ basis set (Table 1). This result is very significant, since the amount of computer time required for these calculations can be more than ten times shorter when using the smaller Pople basis set compared to the bigger

Table 1 Interaction energies (in kJ/mol) for non-covalent dimers **1–10** calculated with different methods

Method	Basis set	Non-covalent dimer									
		1	2	3	4	5	6	7	8	9	10
B3LYP	6-311++G(d,p)	18.15	18.08	20.17	15.25	25.07	11.58	10.06	7.77	10.84	8.10
	6-311++G(3df,3pd)	17.75	17.72	19.77	14.95	24.71	11.66	10.22	8.10	10.99	8.51
	aug-cc-pVDZ	17.86	17.79	19.82	15.03	24.67	11.52	10.08	8.00	10.72	8.31
	cc-pVTZ	17.53	17.72	19.66	14.70	24.57	11.37	9.95	7.91	10.66	8.29
M06-2X	6-311++G(d,p)	-0.89	-1.24	-0.13	-3.38	7.52	-16.30	-17.79	-20.10	-14.41	-16.93
	6-311++G(3df,3pd)	-0.91	-1.21	-0.16	-3.31	7.40	-15.55	-16.90	-18.96	-13.69	-15.85
	aug-cc-pVDZ	-1.45	-1.75	-0.59	-3.68	6.96	-15.93	-17.33	-19.33	-14.02	-16.15
	cc-pVTZ	-0.32	-0.63	0.42	-2.73	7.94	-14.30	-15.69	-17.76	-12.53	-14.69
ωB97X-D	6-311++G(d,p)	-7.86	-8.17	-7.26	-8.62	0.67	-22.65	-23.91	-26.05	-18.33	-20.64
	6-311++G(3df,3pd)	-7.76	-8.02	-7.12	-11.60	0.82	-21.98	-23.14	-25.09	-17.67	-19.69
	aug-cc-pVDZ	-7.79	-8.09	-7.14	-8.44	0.75	-22.22	-23.43	-25.35	-17.96	-19.97
	cc-pVTZ	-7.53	-7.78	-6.83	-8.25	1.12	-21.46	-22.63	-24.55	-17.19	-19.17
B97-D3	6-311++G(d,p)	-7.36	-7.74	-7.15	-5.31	-2.97	-18.54	-19.33	-21.42	-14.43	-16.44
	6-311++G(3df,3pd)	-7.70	-8.12	-7.70	-5.73	-3.56	-18.28	-19.25	-21.05	-14.35	-16.02
	aug-cc-pVDZ	-7.57	-8.16	-7.49	-5.31	-3.31	-18.41	-19.50	-21.25	-14.48	-16.40
	cc-pVTZ	-8.33	-8.79	-8.37	-5.94	-3.85	-18.83	-19.83	-21.71	-14.73	-16.36
OPLS-2005	N/A	5.87	6.53	11.98	7.88	19.13	-12.82	-13.59	-15.24	-8.35	-10.93
OPLS-2005, $\epsilon = 4^a$	N/A	5.02	6.56	12.37	7.63	19.68	-10.90	-10.39	-10.01	-6.21	-6.06
M06-2X, $\epsilon = 4^a$	6-311++G(3df,3pd)	2.95	2.53	2.52	2.33	5.21	-11.03	-11.85	-13.90	-10.42	-9.56
B97-D3, $\epsilon = 4^a$	6-311++G(3df,3pd)	-1.23	-1.35	-1.00	-0.11	2.33	-13.60	-14.16	-15.61	-10.45	-10.10

^a Implicit solvent calculation with dielectric constant $\epsilon = 4$

Pople basis set or the Dunning basis set. It is obvious that these calculations could be performed without large demands in computer strength and time, while still yielding reliable and accurate energy data.

Nevertheless, despite the results from the presented calculations of non-covalent interactions, showing attractive forces between proline and the aromatic part of the ligand in the binding site, the possibility of different protonation states of ionizable groups of the ligand under physiological conditions must be taken into account. For instance, in non-covalent dimers with proline formed with 7-chloro-*N*-methylquinolin-4-amine (**A1**), *N*-methylquinolin-4-amine (**A2**), and *N*-methylpyridin-4-amine (**A4**) (dimers **1**, **2**, **4**, **6**, **7**, and **9**), an aromatic nitrogen atom is involved in the interactions. These molecules could easily be protonated under physiological conditions. The calculated pK_a value for **A1** is 7.99 ± 1.12 , for **A2** 9.08 ± 0.86 , and for **A4** 9.33 ± 1.47 . This clearly indicates that structures **A2** and **A4** under physiological conditions would exist predominantly in their protonated form, which alters their electrostatic properties significantly and could lead to unfavorable interactions with proline in the protein binding site. Significant changes in the electrostatic potential (ESP) could be seen from the representation of electrostatic

potential of neutral and protonated forms of **A1**, **A2**, and **A4** (Fig. 6).

If these ESP maps are compared with the ESP map of **B** (Fig. 7), it could be seen that the non-protonated structures have electrostatic surfaces that would lead to stabilizing electrostatic interaction in the conformations examined in this work. The ESP maps on aromatic non-protonated moieties show slightly negative potential on the surfaces oriented towards **B**, while **B** possess a positive ESP in the zone oriented toward the aromatic rings. Incompatible ESPs would increase electrostatic repulsive interactions in the investigated dimers, thereby considerably lowering the non-covalent stabilization or producing repulsive interactions between two molecules or molecule parts. This was confirmed by our calculations (Supplementary Material, Fig. S1 to S3, Table S1). From that table it can be seen that in this case, calculations of non-covalent interactions by FFs were generally correct for charged systems, but they tend to overestimate the strength of the repulsive interactions (Supplementary Material, Table S1).

Despite having a pK_a value of 7.99 ± 1.12 , meaning that in the unbound state the protonated form of **A1** would be present in larger percent in equilibrium, in given pH range (pH 7.0 ± 2.0), it is very likely that energetically

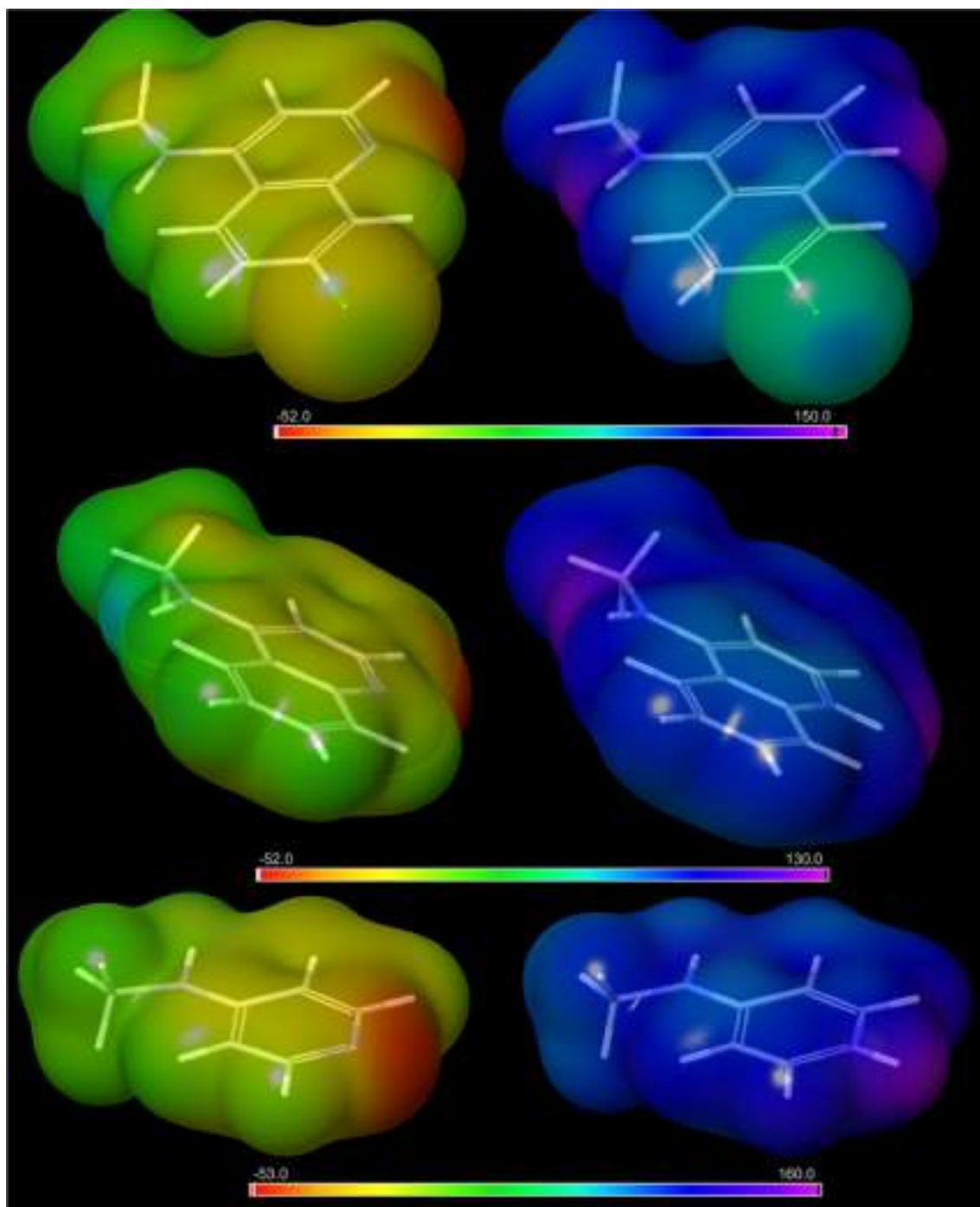


Fig. 6 ESP surfaces of **A1**, **A2**, and **A4** (top to bottom) in non-protonated (left) and protonated (right) form. ESP surfaces were made by mapping electrostatic potential on electron density isosurface

favorable for this structure would be occurrence of predominantly non-protonated form stabilized in ligand–protein complex. This indicates that, regardless of calculated interaction forces between the aromatic moieties and proline, only structures having **A1**, **A3**, and **A5** groups would bind to the protein target under physiological conditions.

All these calculations were performed in gas phase, so we wanted to understand how and to what extent the protein environment would affect the strength of these interactions. Recent theoretical studies of the polar hydrogen– π interactions in protein side chains showed that the presence of the dielectric continuum would lead to decrease in bonding energies for dielectric constant value

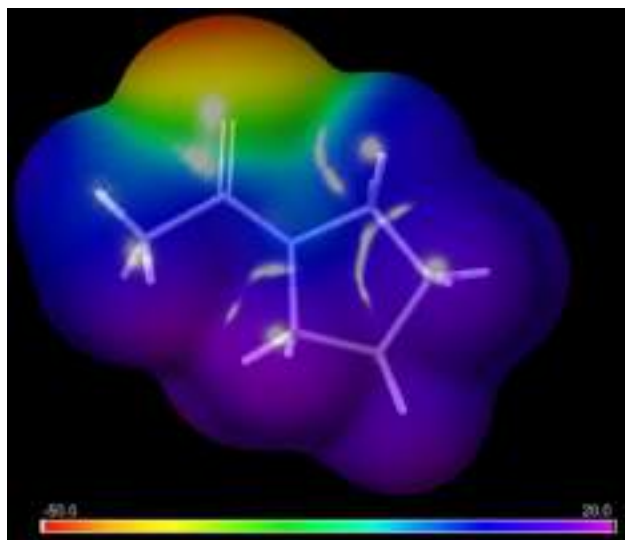


Fig. 7 ESP surface of **B**

of $\epsilon = 2$ [20]. To illustrate the effect of the protein environment, additional calculations were performed in a dielectric continuum employing the most commonly used dielectric constant value of $\epsilon = 4$, which is believed to account for electronic polarization and small backbone fluctuations in proteins [21] (Table 1; Supplementary Material, Table S1). Calculated interaction energies were decreased as expected, while giving the same qualitative picture as gas phase calculations. The presence of the dielectric continuum has the largest influence on non-protonated species, decreasing calculated interaction values up to 6.80 kJ/mol. Protonated forms (**11–16**, Supplementary Material, Table S1), already showing repulsive interactions, were less affected (up to 2.20 kJ/mol).

Conclusions

Besides the usual properties, it is obvious that the presence of proline in the vicinity of aromatic rings can result in stable non-covalent interactions in a way similar to that already known π - π or alkyl- π interactions. This favorable interaction is most probably the outcome of the conformational specificity of the cyclic pyrrolidine structure of proline, permitting larger numbers of dispersive contacts with aromatic moieties. According to the obtained results, and in agreement with previous findings [7], these interactions could be as large as 25 kJ/mol or more (depending on the mutual positions of proline and the aromatic system). This indicates the necessity of the inclusion of this type of interactions in future force field parameterization, as they could influence the positioning and binding strength of a ligand in the binding site of a protein or the docking

score in molecular docking experiments. Thus, when determining the best binding position of ligand in the binding site where this kind of interactions are possible, taking the possible attractive forces into account would probably lead to better docking poses. Until new force fields are developed, to gain a better positioning, these forces could be simulated using small constraints on the related positions of proline and aromatic rings of the ligand. It was shown that these interactions could be calculated using DFT methods, such as ω B97X-D or B97-D3, even with smaller basis sets, without extensive cost in computer time and/or strength. However, the nature of the aromatic group interacting with proline and the protein environment can influence intramolecular non-covalent interactions and must be borne in mind when attempting to determine their extent.

Methods

All calculations were performed using Gaussian 09 [22] and Jaguar from the Schrödinger Suite 2012 [23]. Visualizations were performed using Maestro 9.3 viewer [24] and Chemcraft [25]. All reported binding energies were corrected for the basis set superposition error using the counterpoise method of Boys and Bernardi [26]. Calculations in Gaussian 09 were performed using following keywords combination: #p METHOD/BASIS_SET nosym scf = tight counterpoise = 2. Calculations in Jaguar were performed using the Counterpoise module. All calculations were performed using fixed coordinates of all atoms. This approach was decided on after comparison of the results from test calculations interaction energies in conformations obtained with fixed heavy atoms to all atoms fixed conformations (Supplementary Material, Table S2). The largest difference in energies was 0.22 kJ/mol while the calculations were performed up to 30 % faster. Gaussian calculations were performed using a 32-bit system, employing 4 processors with the %Nproc-Share = 4 keyword. Calculations in Jaguar were performed on the same computer system, using the Windows version of Jaguar, with no ability to use multiple nodes. The pK_a values were obtained using Epik from the Schrödinger Suite 2012 [27]. Molecular mechanic calculations were performed using MacroModel from the Schrödinger Suite 2012 [28].

To find a crystal structure with similar positions of proline and an aromatic moiety, the PDBeMotif service was used [29]. As a search term aromatic moiety with proline in environment was used. As a result, 152 structures were received from the crystal database, which were subjected to a thorough visual check to find the one most similar to our model system.

Calculations with B3LYP [13], M06-2X [18], and ω B97X-D [17] were performed in Gaussian 09, using 4 basis sets: 6-311++G(d,p), 6-311++G(3df,3pd), cc-PVTZ and aug-cc-PVDZ. Jaguar software was used for the B97-D3 [30] calculations. M06-2X is a hybrid meta-GGA functional parameterized in such a manner that it can calculate dispersive interactions [18]. It performs very well at distances of ≈ 5 Å, but according to some authors, the correlation energy tends to fall on longer distances, not showing the correct R-6 behavior [19]. ω B97X-D is a functional developed by Chai and Head-Gordon [17] as a member of a family of long-range corrected (LC) functionals around Becke's B97 mathematical form [31]. It includes 100 % of long-range interactions and about 22 % of short range interactions, modified B97 exchange functional and empirical correction for dispersive interactions. The presence of -D term tends to shift upward the inter-electronic distances over which exact exchange is appropriate. Further improvement is possible using refined DFT-D3 methods [30], which, besides the term varying with R-6, include an R-8 term in the dispersion series. In accordance with the recommendations and conclusions from previous works, B97-D3 [16, 19, 31] was used as a representative of DFT-D3 functionals.

Acknowledgments This research was supported by (1) the Ministry of Education, Science and Technological Development of the Republic of Serbia (Grant No. 172055) and (2) NATO's Public Diplomacy Division in the framework of "Science for Peace" project SfP983638. The authors wish to thank Prof. Dušan Sladić for his help in preparing this manuscript.

References

1. Greaves RB, Warwicker J (2007) *BMC Struct Biol* 7:18
2. Nilsson IM, Sääf A, Whitley P, Gafvelin G, Waller C, von Heijne G (1998) *J Mol Biol* 284:1165
3. Arnold S, Curtiss A, Dean DH, Alzate O (2001) *FEBS Lett* 490:70
4. Yun RH, Anderson A, Hermans J (1991) *Proteins* 10:219
5. Consler TG, Tsolas O, Kaback HR (1991) *Biochemistry* 30:1291
6. Riley KE, Cui G, Merz KM Jr (2007) *J Phys Chem B* 111:5700
7. Biedermannova L, Riley KE, Berka K, Hobza P, Vondrasek J (2008) *Phys Chem Chem Phys* 10:6350
8. <http://www.rcsb.org/pdb/explore.do?structureId=112y>. Accessed 9 Oct 2013
9. Paton RS, Goodman JM (2009) *J Chem Inf Model* 49:944
10. Jorgensen WL, Schyman P (2012) *J Chem Theory Comput* 8:3895
11. Burnett JC, Opsenica D, Sriraghavan K, Panchal RG, Ruthel G, Hermone AR, Nguyen TL, Kenny TA, Lane DJ, McGrath CF, Schmidt JJ, Vennerstrom JL, Gussio R, Šolaja BA, Bavari S (2007) *J Med Chem* 50:2127
12. <http://www.rcsb.org/pdb/explore.do?structureId=2XPU>. Accessed 9 Oct 2013
13. Stephens PJ, Devlin FJ, Chabalowski CF, Frisch MJ (1994) *J Phys Chem* 98:11623
14. Wiberg KB (2004) *J Comput Chem* 25:1342
15. Banks JL, Beard HS, Cao Y, Cho AE, Damm W, Farid R, Felts AK, Halgren TA, Mainz DT, Maple JR, Murphy R, Philipp DM, Repasky MP, Zhang LY, Berne BJ, Friesner RA, Gallicchio E, Levy RM (2005) *J Comput Chem* 26:1752
16. Riley KE, Pitoňák M, Jurečka P, Hobza P (2010) *Chem Rev* 110:5023
17. Chai JD, Head-Gordon M (2008) *Phys Chem Chem Phys* 10:6615
18. Zhao Y, Truhlar DG (2008) *Theor Chem Acc* 120:215
19. Burns LA, Vázquez-Mayagoitia A, Sumpter BG, Sherrill CD (2011) *J Chem Phys* 134:084107
20. Du QS, Wang QY, Du LQ, Chen D, Huang RB (2013) *Chem Cent J* 7:92
21. Gilson MK, Honig B (2004) *Proteins Struct Funct. Bioinf* 4:7
22. Frisch MJ, Trucks GW, Schlegel HB, Scuseria GE, Robb MA, Cheeseman JR, Scalmani G, Barone V, Mennucci B, Petersson GA, Nakatsuji H, Caricato M, Li X, Hratchian HP, Izmaylov AF, Bloino J, Zheng G, Sonnenberg JL, Hada M, Ehara M, Toyota K, Fukuda R, Hasegawa J, Ishida M, Nakajima T, Honda Y, Kitao O, Nakai H, Vreven T, Montgomery Jr JA, Peralta JE, Ogliaro F, Bearpark M, Heyd JJ, Brothers E, Kudin KN, Staroverov VN, Kobayashi R, Normand J, Raghavachari K, Rendell A, Burant JC, Iyengar SS, Tomasi J, Cossi M, Rega N, Millam NJ, Klene M, Knox JE, Cross JB, Bakken V, Adamo C, Jaramillo J, Gomperts R, Stratmann RE, Yazyev O, Austin AJ, Cammi R, Pomelli C, Ochterski JW, Martin RL, Morokuma K, Zakrzewski VG, Voth GA, Salvador P, Dannenberg JJ, Dapprich S, Daniels AD, Farkas Ö, Foresman JB, Ortiz JV, Cioslowski J, Fox DJ, Wallingford CT (2009) *Gaussian 09, Revision A.02*. Gaussian Inc., Pittsburgh
23. Jaguar, version 7.9 (2012) Schrödinger. LLC, New York
24. Maestro, version 9.3 (2012) Schrödinger. LLC, New York, NY
25. <http://www.chemcraftprog.com>. Accessed 9 Oct 2013
26. Boys SF, Bernardi F (1970) *Mol Phys* 19:553
27. Epik, version 2.3 (2012) Schrödinger. LLC, New York
28. MacroModel, version 9.9 (2012) Schrödinger. LLC, New York
29. Golovin A, Henrick K (2008) *BMC Bioinform* 9:312
30. Grimme S, Antony J, Ehrlich S, Krieg H (2010) *J Chem Phys* 132:154104
31. Becke AD (1997) *J Chem Phys* 107:8554